

Structure Exploring, IR and UV Spectroscopic Properties of Pomalidomide as a Second-generation of Immunomodulatory Agent

Reza Ghiasi^{*1}, Rahimeh Rasouli², Farrzaneh Zaaeri³, Fatemeh Ebrahimi Shaghghi⁴

¹*Department of Chemistry, Faculty of science, East Tehran branch, Islamic Azad university, Qiam Dasht, Tehran, Iran*

²*Department of Medical Nanotechnology, International Campus, Tehran University of Medical Sciences, Tehran, Iran*

³*Department of pharmaceutics, Faculty of pharmacy, Tehran University of medical sciences, Tehran, Iran*

⁴*Department of Biology, Science and Research Branch, Islamic Azad University, Tehran, Iran*

(Received 02 Sep. 2016; Final version received 19 Dec. 2016)

Abstract

In this article, the optimized geometry, IR and UV spectra, frontier orbital analysis, natural bond orbital (NBO) analyses, and thermodynamic parameters of pomalidomide were investigated. The calculated structural parameters and stretching frequencies values are compared with experimental values of the investigated compound. Also, the relations of the thermodynamic functions vs. temperatures were fitted by quadratic formulas.

Keywords: *Pomalidomide, Dipole moments, Molecular orbital analysis, Hyperpolarizability, Natural bond analysis (NBO).*

***Corresponding author:** Reza Ghiasi, Department of Chemistry, Faculty of science, East Tehran branch, Islamic Azad University, Qiam Dasht, Tehran, Iran. Email: rezaghiasi1353@yahoo.com, rghiasi@iauet.ac.ir.

Introduction

The successful treatment for multiple myeloma patients stays as a large challenge in multiple myeloma. Average patients' survival has improved with introducing of novel agents such as Thalidomide and lenalidomide [1-6]. Thalidomide and lenalidomide regimens are immunomodulatory agents have commonly used in the treatment of patients with multiple myeloma and caused improvement median survival rate and remissions [7, 8]. Refractory to thalidomide, lenalidomide, and bortezomib therapy, progression and relapse are the greatest challenges in front of multiple myeloma. So, new treatment options are immediately needed for patients with relapsed multiple myeloma.

Second-generation immunomodulatory agent is Pomalidomide. Pomalidomide as a newer Immunomodulatory agent is showing promising results in has shown clinical activity lonely and in combination. Recently it was approved by US Food and Drug Administration (FDA) in February 2013 for treating patients with multiple myeloma who have had at least two therapies with lenalidomide and bortezomib. It was have shown that the disease progressed. It could be more potent and less toxic than thalidomide and lenalidomide, pomalidomide uses orally like thalidomide and lenalidomide and had rapid response. Skin rash was rarely seen with pomalidomide while this symptom is commonly seen with lenalidomide and thalidomide [9]. The mechanisms of action of pomalidomide can be classed as direct antitumor effects and antimyeloma gene regulation [10-12]. It has several function such as direct antiproliferative actions on multiple myeloma cells by its ability to inhibit cyclooxygenase-2 production and prostaglandin generation in lipopolysaccharide-stimulated monocytes [7, 13].

The aim of the present study is to illustrate the results from M062X/6-311++G(d,p) calculations for the molecular geometry, stretching frequencies values, conformational, natural bond orbital (NBO) and nonlinear optical (NLO) analyses, highest occupied molecule energy level (EHOMO), the lowest unoccupied molecule energy level (ELUMO), the HOMO-LUMO energy gap (E_g) between EHOMO and ELUMO, hardness (η), chemical potential (μ), thermodynamic parameters, NBO analysis of investigated compound.

Experimental

All calculations were carried out with the Gaussian 09 suite of program [14]. The calculations of systems contain main group elements described by the standard 6-311++G(d,p) basis set [15-18]. Geometry optimization was performed utilizing with the hybrid functional of Truhlar and Zhao (M062X) [19]. A vibrational analysis was performed at each stationary point found, that confirm its identity as an energy minimum. The population analysis has also been performed by the natural

bond orbital method [20] using NBO program [21] under Gaussian 2009 program package. The information of the MOs was evaluated by total, partial and overlap population density of states (DOS) using the GaussSum 3.0 [22].

Results and discussion

Geometric parameters

Figure 1 presents the structure of pomalidomide and the numbering of atoms. The global minimum energy, zero-point vibrational energies, rotational constants, and entropy moments obtained for optimized geometry of pomalidomide in the m062x/6-311++g(d,p) level of theory are presented in Table 1.

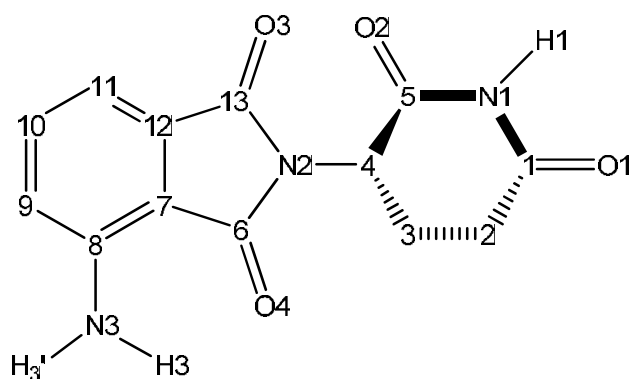


Figure 1. The molecular structure and numbering of atoms in pomalidomide.

Table 1. The some of the calculated parameters of pomalidomide in the m062x/6-311++g(d,p) level of theory.

parameter	value
SCF energy (Hartrees)	-967.1443
Total energy (thermal), E_{total} (kcal mol ⁻¹)	158.634
Heat capacity at const. volume, C_v (cal mol ⁻¹ K ⁻¹)	63.308
Entropy, S (cal mol ⁻¹ K ⁻¹)	129.959
Vibrational energy, E_{vib} (kcal mol ⁻¹)	156.857
Zero-point vibrational energy, E_0 (kcal mol ⁻¹)	148.430
Ionization energy (vertical, eV)	8.57
Ionization energy (adiabatic), eV)	8.29
electron affinity (vertical, eV)	0.85
electron affinity (adiabatic, eV)	1.24
Rotational constants (GHz)	
A	0.9048
B	0.1982
C	0.1817

Bond distances of pomalidomide are collected in Table 2. These values show that theoretical results are close to the experimental values for the title molecule[23]. The minor differences may due to the fact that the theoretical calculations were aimed at the isolated molecule in gaseous phase and the experimental results were aimed at the molecule in the solid state. The calculated geometric parameters also represented good approximation so they could be used as foundation to calculate the other parameters for the compound.

Table 2. The bond distances of pomalidomide in the m062x/6-311++g(d,p) level of theory.

	C1- C2	C2- C3	C3- C4	C4-C5	C6- C7	C7- C8	C7- C12	C8- C9	C9- C10	C10- C11	C11- C12	C12- C13
exp	1.496	1.514	1.514	1.523	1.459	1.397	1.391	1.398	1.374	1.403	1.371	1.488
theo	1.512	1.525	1.527	1.532	1.495	1.393	1.391	1.413	1.386	1.404	1.375	1.473
	C1- O1	C5- O2	C6- O4	C13- O3								
exp	1.216	1.211	1.222	1.211								
theo	1.203	1.204	1.208	1.201								
	C1- N1	C8- N3	C5- N1	N2- C13	N2- C6	N2- C4						
exp	1.379	1.371	1.378	1.395	1.400	1.448						
theo	1.395	1.365	1.386	1.401	1.403	1.440						

IPs and EAs

The ionization potential (IP) and electron affinity (EA) are well defined properties that can be calculated by DFT to estimate electrons into the compounds. These values aim to get an in detail rationalization of the relationship between the structure and the electronic behavior of the molecule, in particular the response of the molecule to the formation of a hole, or to the addition of an electron, additional information is derived. Table 1 contains the calculated IPs, EAs, both vertical and adiabatic, and the extraction potentials (HEP and EEP for the hole and electron, respectively) that refer to the geometry of the ions [24, 25]. The IP and EA can be either for vertical excitations (v, at the geometry of the neutral molecule) or adiabatic excitations (a, optimized structure for both the neutral and charged molecule). The $\lambda_{\text{electron}}$ is electron reorganization energy, which can be expressed as follows:

$$\lambda_{\text{electron}} = \text{EEP} - \text{EA}(\text{v})$$

EEP (electron Extraction potential) is the energy difference from E to E⁻ (anionic), with using E⁻ geometric structure in calculation. Likewise, λ_{hole} for hole transfer can be expressed as follows:

$$\lambda_{\text{hole}} = \text{IP}(\text{v}) - \text{HEP}$$

HEP (hole Extraction potential) is the energy difference from E (neutral molecule) to E⁺ (cationic), with using E⁺ geometric structure in calculation. The mobility of charges has been established to be

related mainly to the internal reorganization energy $\lambda_{\text{hole/electron}}$. The calculations show that the λ_{hole} value (0.511eV) for molecule is less than their corresponding $\lambda_{\text{electron}}$ value (0.722 eV), which indicates that the electron transfer rate is less than the hole transfer rate.

Frontier orbitals energy

It is well-known that the frontier orbitals energy and E_g values are closely related to the optical and electronic properties. To get insight into the influence of the optical and electronic properties, the distributions of the frontier orbitals for these molecules are investigated, and their sketches are plotted in Figure 2. Molecular orbital analysis show that frontier orbitals are of the π characteristics.

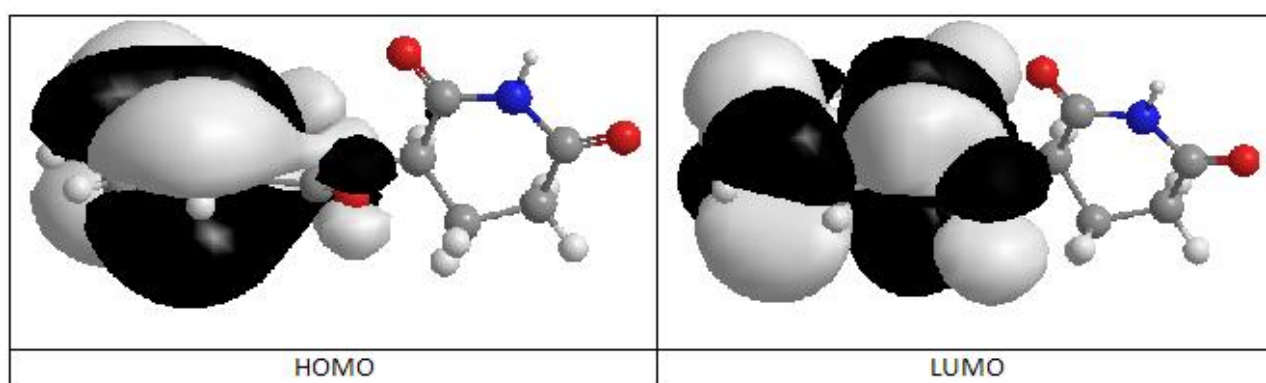


Figure 2. The plots of frontier orbitals in pomalidomide.

Another method to realize the influence of the optical and electronic properties is to analyze the $E(\text{HOMO})$, $E(\text{LUMO})$, and E_g values. The frontier orbital energy and HOMO-LUMO gap in case of pomalidomide are found to be -7.79, -1.58, and 6.21 eV, respectively. To evaluate the electrophilicity of the pomalidomide, we have calculated the electrophilicity index, ω , for each complex measured according to Parr, Szentpaly, and Liu [26] using the expression:

$$\omega = \frac{\mu^2}{2\eta}$$

The global electrophilicity index is the lowering of energy due to maximal electron flow between donor and acceptor, Where μ is the chemical potential (the negative of the electronegativity), and η is the hardness [27, 28]. These values can be calculated from the HOMO and LUMO orbital energies using the following approximate expression:

$$\mu = \frac{E(\text{HOMO}) + E(\text{LUMO})}{2}$$

describing the escaping tendency of electron from a stable system

$$\chi = -\frac{E(\text{HOMO}) + E(\text{LUMO})}{2}$$

$$\eta = \frac{E(\text{LUMO}) - E(\text{HOMO})}{2}$$

which demonstrates the resistance to alteration in electron distribution. The values of hardness, chemical potential and electrophilicity of pomalidomide are 3.10, -4.68, 3.54 eV, respectively. To understand the central features of bonding interactions of compounds, we performed density of states of the total (TDOS, Figure 3).

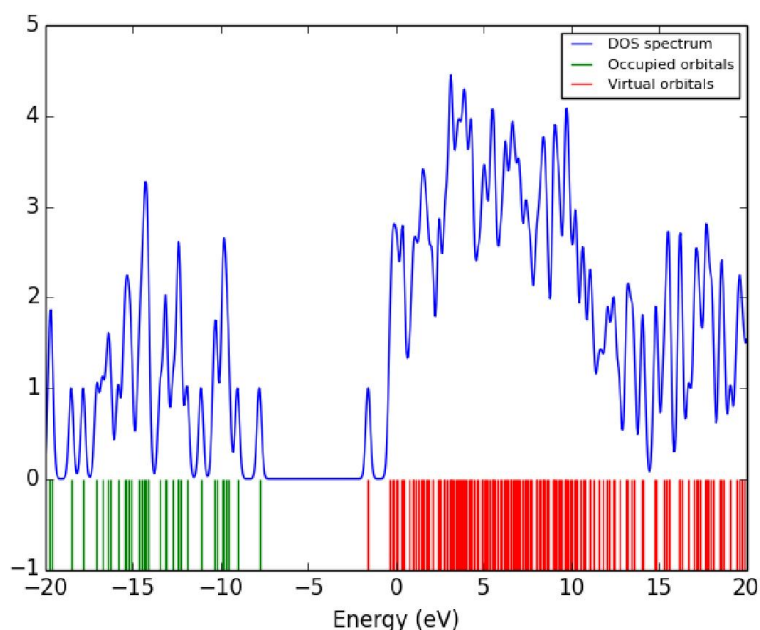


Figure 3. Density of state diagram of pomalidomide.

Dipole moment

The dipole moment of a molecule is a significant property that is essentially used to investigation the intermolecular interactions involving the non-bonded type dipole–dipole interactions, since higher the dipole moment, stronger will be the intermolecular interactions.

The total (static) dipole moment written as:

$$\mu = \sqrt{\mu_x^2 + \mu_y^2 + \mu_z^2}$$

The total dipole moment (μ_{total}) of pomalidomide, and related components (μ_x , μ_y and μ_z) have been calculated using M062x/6-311++G(d,p) level of theory. These calculations show that $\mu_{\text{total}} = 5.42$ Debye. The value I μ_x , μ_y and μ_z are -4.805, 1.88, and -1.66 Debye, respectively.

Polarizability

Polarizability is an important parameters in structural chemistry[29]. This is the measure of the distortion of a molecule in an electric field. For a molecule in an electric field of strength, H, the induced dipole moment, μ , of the molecule would vary proportionally with the field:

$$\mu = \alpha \cdot H$$

The Isotropic and anisotropic polarizability ($\langle \alpha \rangle, \Delta\alpha$) of pomalidomide, and related components ($\alpha_{xx}, \alpha_{yy}, \alpha_{zz}$) have been calculated using M062x/6-311++G(d,p)** level of theory.

$$\langle \alpha \rangle = \frac{(\alpha_{xx} + \alpha_{yy} + \alpha_{zz})}{3}$$

$$\Delta\alpha = \left[\frac{(\alpha_{xx} - \alpha_{yy})^2 + (\alpha_{yy} - \alpha_{zz})^2 + (\alpha_{zz} - \alpha_{xx})^2}{2} \right]^{\frac{1}{2}}$$

These calculations show $\langle \alpha \rangle$ and $\Delta\alpha$ are 179.6 and 111.08 Bohr³, respectively. The value ($\alpha_{xx}, \alpha_{yy}, \alpha_{zz}$) are 246.04, 174.7, and 118.05 Bohr³, respectively.

Hyperpolarizability

Hyperpolarizability is main parameters in structural chemistry[29]. There has been a deep research for molecules with large non-zero hyperpolarizabilities, since these substances have a potential as the first hyperpolarizabilities (β_{total}) of pomalidomide, and related properties (β_x, β_y , and β_z) were calculated using M062X/6-311++G(d,p) level of theory. The total static first hyperpolarizability β was obtained from the relation:

$$\beta_{tot} = \sqrt{\beta_x^2 + \beta_y^2 + \beta_z^2}$$

upon calculating the individual static components

$$\beta_i = \beta_{iii} + \frac{1}{3} \sum_{i \neq j} (\beta_{ijj} + \beta_{jij} + \beta_{jji})$$

Due to the Kleinman symmetry[30]:

$$\beta_{xyy} = \beta_{yyx} = \beta_{yyx} ; \beta_{yyz} = \beta_{zyy} = \beta_{zyy}, \dots$$

one finally obtains the equation that has been employed:

$$\beta_{tot} = \sqrt{(\beta_{xxx} + \beta_{xyy} + \beta_{xzz})^2 + (\beta_{yyy} + \beta_{yzz} + \beta_{yxx})^2 + (\beta_{zzz} + \beta_{zxx} + \beta_{zyy})^2}$$

The first hyperpolarizability of pomalidomide is 3.18×10^{-30} esu. The β_x , β_y , and β_z values of pomalidomide are collected in Table 3. From Table 3, the β_x value dominates the second-order NLO response, because the skeleton atoms mostly locate on the x-axis.

Table 3. β components (10^{-30} esu) and β_{tot} values for pomalidomide in the M 0 62 X / 6-311++G (d,p) level of theory.

β_{XXX}	337.07
β_{XXY}	179.00
β_{XYY}	-25.25
β_{YYY}	-286.67
β_{XXZ}	-49.92
β_{XYZ}	-35.05
β_{YYZ}	-27.51
β_{XZZ}	16.75
β_{VZZ}	-22.57
β_{ZZZ}	-26.33
β_{tot}	3.18×10^{-30}
$\beta_{\text{tot}} \times 10^{30}$	3.18
β_x	2.84×10^{-30}
β_y	-1.12×10^{-30}
β_z	-8.96×10^{-30}

Vibrational spectrum analysis

Figure 4 presents Infra-red spectrum of pomalidomide molecule. The observed IR bands and calculated wavenumbers and assignments are given in Table 4.

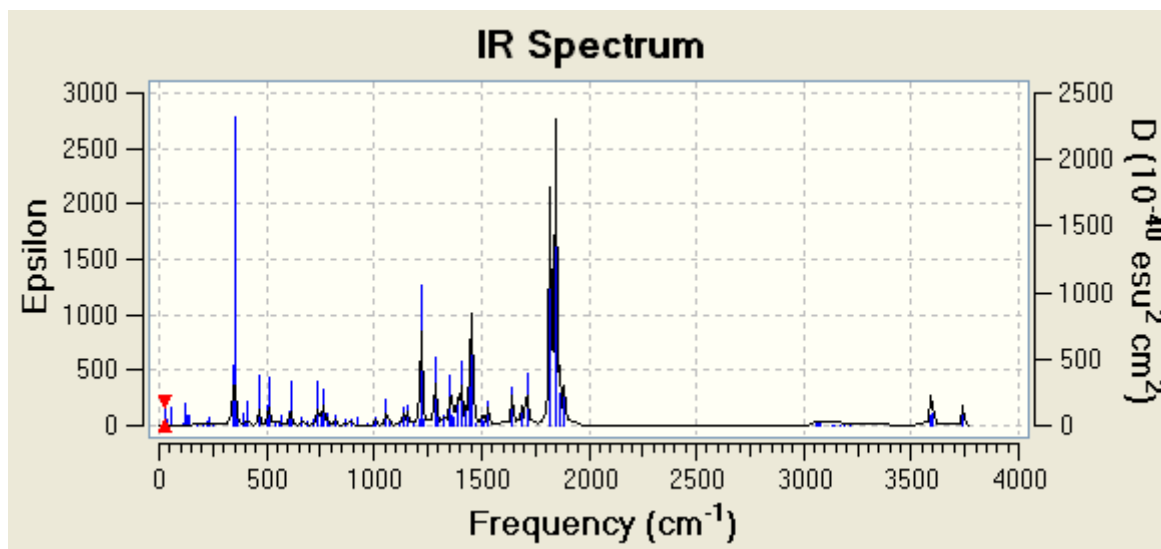
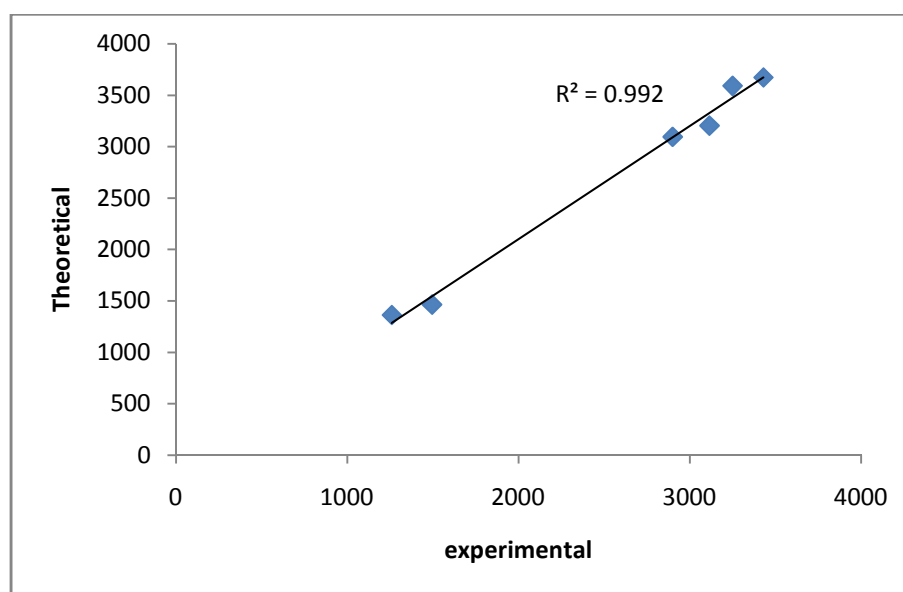


Figure 4. IR spectrum of pomalidomide.

Table 4. The observed IR bands and calculated wavenumbers and assignments for pomalidomide in the m062x/6-311++g(d,p) level of theory.

$\nu(\text{cm}^{-1})$, experimental	$\nu(\text{cm}^{-1})$, theoretical	Functional group
3482, 3378	3741, 3602	Aniline N-H stretching
3250	3590	Imide N-H stretch
3115	3217,3189	Aromatic C-H stretch
2900	3145,3129,3077,3063,3058	Aliphatic C-H stretch
1595,1480,1409	1505,1428,1456	Aromatic C=C stretching
1260	1362	Aniline C-N stretch

The N-H stretching vibrations generally give rise to bands at 3500–3400 cm^{-1} [31, 32].1. In the present study, the N-H stretching band are in 3741, 3602 cm^{-1} in the IR spectrum.The C-N stretching modes are reported in the range 1100–1300 cm^{-1} [33].In the present case the C-N stretching modes are assigned at 1362 cm^{-1} theoretically. The phenyl CH stretching vibrations occur above 3000 cm^{-1} and are typically exhibited as multiplicity of weak to moderate bands compared with the aliphatic CH stretching[34].For the title compound, this calculation gives CH stretching vibrations of the phenyl rings at 3217 and 3189 cm^{-1} . The aliphatic CH stretching vibrations are at 3145,3129,3077,3063, and 3058 cm^{-1} . Figure 5 presents a good relationship between experimental and theoretical wavenumbers.

**Figure 5.** Linear correlation between experimental and theoretical wavenumber in pomalidomide.

Electronic spectra

We found the most intense electronic transition (λ_{\max}) of pomalidomide. The wavelength, oscillator strength and the composition of the transitions obtained by TD-DFT calculations are given in Table 5. Theoretical calculations indicate that, in pomalidomide molecule HOMO-2→LUMO transition makes the major contribution in this electronic transition.

Table 5. The wavelength, oscillator strengths, the composition of the maximum electronic transitions for pomalidomide.

Transition	λ_{\max}	f
HOMO-2→LUMO	205.53	0.4083
HOMO-1→LUMO+3	197.97	0.3205
HOMO-5→LUMO+4	177.80	0.4193
HOMO-8→LUMO	173.16	0.2122

Nucleus Independent Chemical Shift analyses (NICS)

The nucleus-independent chemical shift (NICS) index, based on the magnetic criterion of aromaticity, is probably the most widely used probe for examination of chemical compounds aromatic properties [35]. It is defined as the negative value of the absolute magnetic shielding. It can be calculated in the centre of the aromatic ring (NICS(0) [36]), or at 1 Å above it (NICS(1) [37]). Negative NICS values denote efficient electron delocalization. Nucleus-independent chemical shifts were calculated in the point located by 1 Å above the center of the ring (NICS(1)_{zz}) as it was recommended for obtaining more accurate data [38, 39]. NICS values are calculated using the Gauge independent atomic orbital (GIAO) [40] method at the same method and basis sets for optimization.

A large negative NICS at the ring center (or inside and above the molecular plane) implies the presence of diamagnetic ring currents. The NICS values were calculated using m062x/6-311++G(d,p) level of theory. These calculation show that the computed NICS(0.0) values at the geometrical center of cycle is -7.13 ppm, suggesting these molecules are clearly aromatic. In order to further identify the aromaticity of the molecules, we calculated the NICS values (including NICS(0.5), NICS(1.0), NICS(1.5), and NICS(2.0)) by placing a series of ghost atoms above (by 0.5, 1.0, 1.5, 2.0 Å) the geometrical centers. All these NICS values are mainly attribute to the delocalized π electrons current. These values are -8.67, -8.37, -6.01, -3.82 ppm, respectively. The most negative of these values are 0.5 Å above of the ring center. In addition, we focused on the NICS(0.5)_{zz}, NICS(1.0)_{zz}, NICS(1.5)_{zz} and NICS(2.0)_{zz} indexes to explain the variation of the degree of aromaticity in all ring. These values are -8.92, -15.89, -22.12, -18.80, -13.35 ppm.

NBO analysis

The Natural Bond Orbital (NBO) analysis of molecules has provided the detailed insight into the nature of electronic conjugation between the bonds in this molecule.

Figure 6 depicts the natural charges on atoms. The largest negative charge is located on N1 atom.

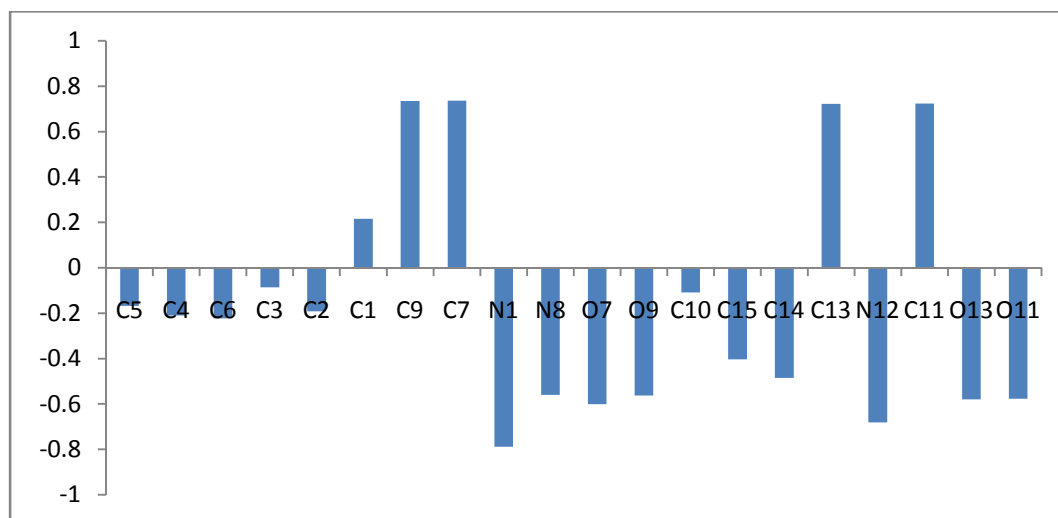


Figure 6. NBO charge distribution in of pomalidomide.

The most important interaction between “filled” (donor) Lewis type NBOs and “empty” (acceptor) non-Lewis NBOs is reported in Table 6. The most charge transfer energies are collected in Table 6. In Table 6 the perturbation energies of significant donor–acceptor interactions are comparatively presented for pomalidomide. The larger the $E(2)$ value, the intense is the interaction between electron donors and electron acceptors.

Table 6. The second-order perturbation energies $E(2)$ (kcal/mol) corresponding to the most important charge transfer interactions (donor \rightarrow acceptor) for pomalidomide.

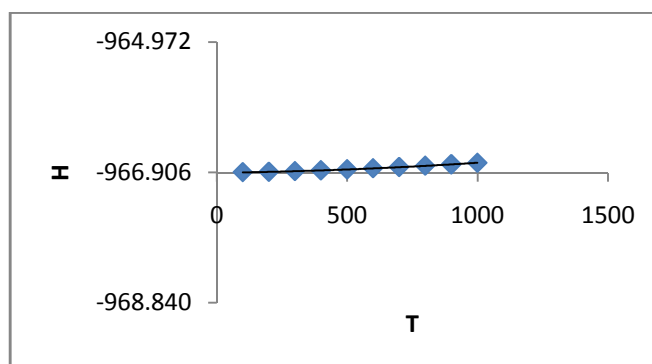
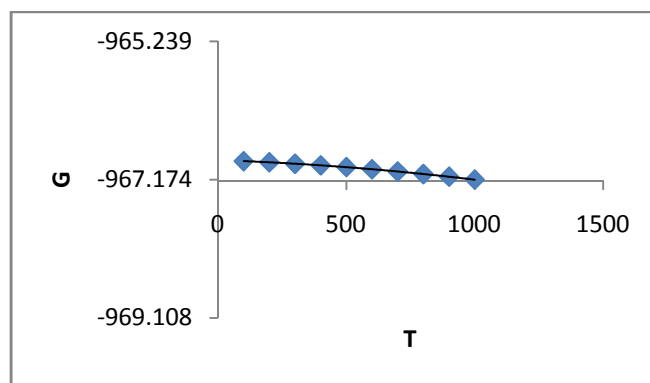
Donor NBO \rightarrow acceptor NBO	$E(2)$	$E(j)-E(i)$	$F(i,j)$
CR (1) N3 \rightarrow BD*(1) N 1 - H 1	482.18	17.86	2.631
CR (1) N3 \rightarrow BD*(1) C 5 - O 2	372.16	17.99	2.315
CR (1) N3 \rightarrow RY*(6) H 3	932.77	15.05	3.345
BD (1) N3 - H3 \rightarrow RY*(6) H 3	696.05	1.17	0.808
BD (1) N11 - H30 \rightarrow RY*(6) H 3	228.84	1.20	0.469
BD (1) C8 - N3 \rightarrow RY*(6) H 3	333.81	1.38	0.608

Thermodynamic properties

The energies and thermodynamic parameters of the compound have also been computed and are presented in Table 1. The frequency calculations compute the zero point energies, thermal

correction to internal energy, enthalpy, Gibbs free energy and entropy as well as the heat capacity for a molecular system were listed in Table 1. The temperature dependence of the thermodynamic properties heat capacity at constant pressure (C_p) and entropy (S) and for pomalidomide were also determined and listed in Table 7. From Table 7, one can find that the entropies, heat capacities, and enthalpy changes are increasing with temperature ranging from 100 to 1000 K due to the fact that the molecular vibrational intensities increase with temperature. These observed relations of the thermodynamic functions vs. temperatures were fitted by quadratic formulas (Figure 7). The corresponding fitting equations for pomalidomide are:

$$\begin{aligned} G &= -2 \times 10^{-7} T^2 - 1 \times 10^{-4} T - 966.9; & R^2 &= 1.0000 \\ H &= 1 \times 10^{-7} T^2 + 5 \times 10^{-5} T - 966.91; & R^2 &= 0.9995 \\ S &= -6 \times 10^{-5} T^2 + 0.2563 T + 58.78; & R^2 &= 1.0000 \\ C_v &= -1 \times 10^{-4} T^2 + 0.2414 T + 1.0396; & R^2 &= 0.9997 \end{aligned}$$



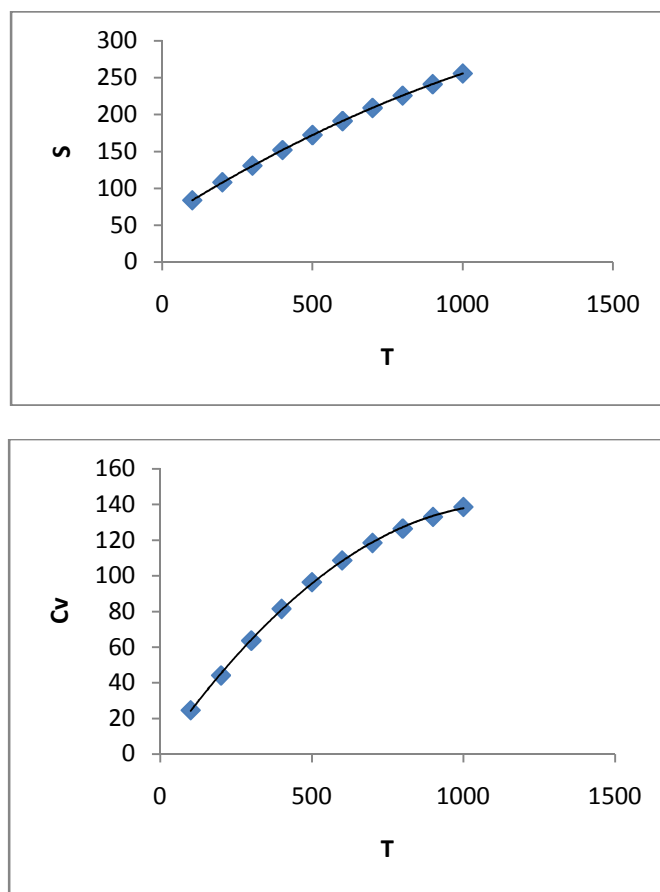


Figure 7. Quadratic temperature dependency of thermodynamic parameters.

Table 7. Standard thermodynamic functions of the pomalidomide.

T	G (Hartree)	H (Hartree)	S (Cal/Mol.K)	C _v (Cal/Mol.K)
100	-966.918	-966.905	83.561	24.651
200	-966.934	-966.899	107.952	44.126
300	-966.953	-966.89	130.365	63.658
400	-966.975	-966.878	151.746	81.441
500	-967.001	-966.864	172.025	96.421
600	-967.03	-966.847	191.081	108.581
700	-967.062	-966.829	208.895	118.401
800	-967.096	-966.809	225.505	126.404
900	-967.134	-966.788	241.02	133.01
1000	-967.173	-966.766	255.538	138.528

Conclusion

In the present study, theoretical study of structure and properties of pomalidomide was examined. The optimized geometrical parameters of the molecules obtained in the M062X/6-311++G(d,p) level of theory revealed:

1. The vibrational spectrum analysis presents a good relationship between experimental and theoretical wavenumbers.
2. TD-DFT calculation exhibits HOMO-2→LUMO transition makes the major contribution in the most intensity of electronic transition.
3. The most negative values of NICS above of the rings reveals π -aromaticity in six-member ring.
4. NBO analysis shows that largest negative charge is located on N1 atom.

Acknowledgment

The authors would like to thank Department of Medical Nanotechnology, School of Medicine, International Campus and Tehran University of Medical Sciences for a generous donation of computational time.

References

- [1] M. Dimopoulos, A. Spencer, M. Attal, H. M. Prince, J.-L. Harousseau, A. Dmoszynska, J. S. Miguel, A. Hellmann, T. Facon, R. Foà, *New England Journal of Medicine*, 357 (2007).
- [2] S. Rajkumar, M. Gertz, M. Lacy, A. Dispenzieri, R. Fonseca, S. Geyer, N. Iturria, S. Kumar, J. Lust, R. Kyle, *Leukemia*, 17 (2003).
- [3] S. V. Rajkumar, S. Jacobus, N. S. Callander, R. Fonseca, D. H. Vesole, M. E. Williams, R. Abonour, D. S. Siegel, M. Katz, P. R. Greipp, *The lancet oncology*, 11 (2010).
- [4] S. Singhal, J. Mehta, R. Desikan, D. Ayers, P. Roberson, P. Eddlemon, N. Munshi, E. Anaissie, C. Wilson, M. Dhodapkar, *New England Journal of Medicine*, 341 (1999).
- [5] D. M. Weber, C. Chen, R. Niesvizky, M. Wang, A. Belch, E. A. Stadtmauer, D. Siegel, I. Borrello, S. V. Rajkumar, A. A. Chanan-Khan, *New England Journal of Medicine*, 357 (2007).
- [6] S. K. Kumar, S. V. Rajkumar, A. Dispenzieri, M. Q. Lacy, S. R. Hayman, F. K. Buadi, S. R. Zeldenrust, D. Dingli, S. J. Russell, J. A. Lust, *Blood*, 111 (2008).
- [7] P. G. Richardson, T. M. Mark, M. Q. Lacy, *Critical reviews in oncology/hematology*, 88, (2013).
- [8] N. Saini, A. Mahindra, *Expert opinion on investigational drugs*, 22 (2013).
- [9] M. Q. Lacy, A. R. McCurdy, *Blood*, 122 (2013).
- [10] L. Escoubet-Lozach, I.-L. Lin, K. Jensen-Pergakes, H. A. Brady, A. K. Gandhi, P. H. Schafer, G. W. Muller, P. J. Worland, K. W. Chan, D. Verhelle, *Cancer research*, 69 (2009).
- [11] S. Li, R. Pal, S. A. Monaghan, P. Schafer, H. Ouyang, M. Mapara, D. L. Galson, S. Lentzsch, *Blood*, 117 (2011).

- [12] D. Verhelle, L. G. Corral, K. Wong, J. H. Mueller, L. Moutouh-de Parseval, K. Jensen-Pergakes, P. H. Schafer, R. Chen, E. Glezer, G. D. Ferguson, *Cancer research*, 67 (2007).
- [13] G. D. Ferguson, K. Jensen-Pergakes, C. Wilkey, U. Jhaveri, N. Richard, D. Verhelle, L. M. De Parseval, L. G. Corral, W. Xie, C. L. Morris, *Journal of clinical immunology*, 27 (2007).
- [14] M. J. Frisch, G. W. Trucks, H. B. Schlegel, G. E. Scuseria, M. A. Robb, J. R. Cheeseman, G. Scalman, V. Barone, B. Mennucci, G. A. Petersson, H. Nakatsuji, M. Caricato, X. Li, H. P. Hratchian, A. F. Izmaylov, J. Bloino, G. Zheng, J. L. Sonnenberg, M. Hada, M. Ehara, K. Toyota, R. Fukuda, J. Hasegawa, M. Ishida, T. Nakajima, Y. Honda, O. Kitao, H. Nakai, T. Vreven, J. A. Montgomery, Jr., J. E. Peralta, F. Ogliaro, M. Bearpark, J. J. Heyd, E. Brothers, K. N. Kudin, V. N. Staroverov, R. Kobayashi, J. Normand, K. Raghavachari, A. Rendell, J. C. Burant, S. S. Iyengar, J. Tomasi, M. Cossi, N. Rega, J. M. Millam, M. Klene, J. E. Knox, J. B. Cross, V. Bakken, C. Adamo, J. Jaramillo, R. Gomperts, R. E. Stratmann, O. Yazyev, A. J. Austin, R. Cammi, C. Pomelli, J. W. Ochterski, R. L. Martin, K. Morokuma, V. G. Zakrzewski, G. A. Voth, P. Salvador, J. J. Dannenberg, S. Dapprich, A. D. Daniels, O. Farkas, J. B. Foresman, J. V. Ortiz, J. Cioslowski, D. J. Fox, Revision A.02 ed., Gaussian, Inc., Wallingford CT(2009).
- [15] R. Krishnan, J. S. Binkley, R. Seeger, J. A. Pople, *J. Chem. Phys.* , 72, 650 (1980).
- [16] A. J. H. Wachters, *J. Chem. Phys.*, 52, 1033 (1970).
- [17] P. J. Hay, *J. Chem. Phys.* , 66, 4377 (1977).
- [18] A. D. McLean, G. S. Chandler, *J. Chem. Phys.*, 72, 5639 (1980).
- [19] Y. Zhao, D. G. Truhla, *J. Phys. Chem*, 110, 5121 (2006).
- [20] A. E. Reed, L. A. Curtiss, F. Weinhold, *Chem. Rev.* , 88, 899 (1988).
- [21] E. D. Glendening, A. E. Reed, J. E. Carpenter, F. Weinhold, 3.1. ed., Gaussian Inc, Pittsburg, PA, 2003.
- [22] N. M. O'Boyle, A. L. Tenderholt, K. M. Langner, *J. Comp. Chem.*, 29, 839 (2008).
- [23] G. W. Muller, D. I. Stirling, R. S.-C. Chen, Google Patents(1997).
- [24] A. Curioni, M. Boero, W. Andreoni, *Chem Phys Lett.*,294, 263 (1998).
- [25] I. Wang, E. Botzung-Appert, O. S. p. O, A. Ibanez, P. L. Baldeck, *J Opt A Pure Appl Opt.*,4, S258 (2002).
- [26] R. G. Parr, v. S. I. L, S. Liu, *J. Am. Chem. Soc.*, 121, 1922 (1999).
- [27] R. G. Pearson, *Chemical Hardness*, Wiley-VCH: Oxford(1997).
- [28] R. G. Parr, W. Yang, *Density-Functional Theory of Atoms and Molecules*, Oxford University Press: New York (1989).
- [29] D. Avci, A. Basoglu, Y. Atalay, *Int. J. Quant. Chem.*, 111, 130 (2011).
- [30] D. A. Keleiman, *Phy. Rev*, 126, 1977 (1962).

- [31] A. Spire, M. Barthes, H. Kallouai, G. DeNunzio, *Physics*, D137, 392 (2000).
- [32] L. J. Bellami, *The IR Spectra of Complex Molecules*, John Wiley and Sons, New York (1975).
- [33] S. Kundoo, A. N. Banerjee, P. Saha, K. K. Chattophyay, *Mater. Lett.*, 57, 2193 (2003).
- [34] i. R. A. M. E. J. Coates, *Interpretation of Infrared Spectra, A Practical Approach*, John Wiley and Sons Inc., Chichester(2000).
- [35] Z. Chen, C. S. Wannere, C. Corminboeuf, R. Puchta, P. v. R. Schleyer, *Chem. Rev*, 105, 3842 (2005).
- [36] P. v. R. Schleyer, C. Marker, A. Dransfeld, H. Jiao, N. J. R. V. Hommes, *J. Am. Chem. Soc.*, 118, 6317 (1996).
- [37] P. v. R. Schleyer, M.Monohar, Z. Wang, B. Kiran, H. Jiao, R. Puchta, N. J. R. V. Hommes, *Org. Lett*, 3, 2465 (2001).
- [38] C. Corminboeuf, T. Heine, G. Seifert, P. v. R. Schleyer, J. Weber, *Phys. Chem. Chem. Phys*, 6, 273 (2004).
- [39] H. Fallah-Bagher-Shaidaei, C. S. Wannere, C. Corminboeuf, R. Puchta, P. v. R. Schleyer, *Org. Lett*, 8, 863 (2006).
- [40] K. Wolinski, J. F. Hinton, P. Pulay, *J. Am. Chem. Soc.*, 112, 8251 (1990).